Energy Absorption of Multi-Material Cellular Structures

by

Rajeshree Pawan Varma

A Thesis Presented in Partial Fulfillment
of the Requirements for the Degree
Master of Science

Approved April 2021 by the
Graduate Supervisory Committee:

Dhruv Bhate, Chair
Qiong Nian
Abdelrahman Shuaib

ARIZONA STATE UNIVERSITY

May 2021

ABSTRACT

Inspired by the design of lightweight cellular structures in nature, humans have made cellular solids for a wide range of engineering applications. Cellular structures composed of solid and gaseous phases, and an interconnected network of solid struts or plates that form the cell's edges and faces. This makes them an ideal candidate for numerous energy absorption applications in the military, transportation, and automotive industries. The objective of the thesis is to study the energy-absorption of multi-material cellular structures. Cellular structures made from Acrylonitrile-Butadiene-Styrene (ABS) a thermoplastic polymer and Thermoplastic Polyurethane (TPU) a thermoplastic elastomer were manufactured using dual extrusion 3D printing. The surface-based structures were designed with partitions to allocate different materials using Matlab and nTopology. Aperiodicity was introduced to the design through perturbation. The specimens were designed for two wall thicknesses - 0.5mm and 1mm, respectively. In total, 18 specimens were designed and 3D printed. All the specimens were tested under quasi-static compression. A detailed analysis was performed to study the energy absorption metrics and draw conclusions, with emphasis on specific energy absorbed as a function of relative density, efficiency, and peak stress of the specimens to hypothesize and validate mechanisms for observed behavior. All the specimens were analyzed to draw comparisons across designs.

DEDICATION

Life does not always give you second chances. From August 2019 to late 2020, for more than a year, I have been struggling with health issues. It was because of the support of my loved ones I am able to get back on my feet and write this document today. With deep love and affection, I dedicate this thesis to my friends who have become family, and of course my parents and family. It is their unconditional love and support that has always cheered me up. This Master's degree and thesis would not have been possible without them. I am grateful to my parents for letting me fulfil my dream of pursuing higher education in the United States . I made a promise to make my parents proud by achieving my master's degree and I hope that I have fulfilled my promise. Thank you for your endless unconditional love, sacrifices, prayers , advice, and support .

ACKNOWLEDGMENTS

I would like to express my deepest appreciation to my committee chair, Dr. Dhruv Bhate, who guided me through my graduate education and shared the excitement of his discovery on biomaterials. Without his guidance and persistent help this thesis would not have been possible.

I want to appreciate Daniel Anderson for the design and laying the groundwork of this project. Daniel has always helped me and shared his insights with me. In addition, I would like to thank Dr. Prince Jeya Lal Lazar for the thorough discussions and help with testing and support. Irving Ramirez and Mandar Shinde for help through testing and analysis and all the other members of 3DX Research group for their support and contribution during the thesis.

TABLE OF CONTENTS

Page

LIST OF FIGURES

Figure Page

Figure Page

CHAPTER 1

INTRODUCTION

1.1 Introduction

Additive Manufacturing is defined as a material joining process, whereby a product can be directly fabricated from its 3D model [1]. In conventional manufacturing processes like casting and molding, milling, turning, etc. excess material is removed to achieve the final product. In additive manufacturing the product is built layer by layer. Additive Manufacturing (AM) processes have some benefits over conventional manufacturing processes. First, parts with complex geometries can be fabricated without significantly increasing the production cost. Second, parts with different material compositions can be manufactured using multi-material AM processes. Third, as the part is directly printed from the 3D model, manufacturing preparation time can be reduced [1]. Because of these unique features of additive manufacturing technologies, they are widely used in industries like aerospace, automotive, defense and biomedical industry.

1.2 What is a Cellular Solid ?

The word cell comes from the Latin word ‘cella’, meaning a small compartment [2]. A cellular solid is a cellular structure composed of solid and gaseous phases. They consist of an interconnected network of solid struts or plates that form the cell’s edges and faces [3]. Cork, nacre, wood, and sponge are some common cellular structures found in nature. These structures have low density, high specific strength, and high energy absorption which can inspire the design of many

novel structures with high energy absorption applications [4]. According to the geometric configuration of each cell unit, cellular structures can be grouped into three categories - stochastic foams, prismatic honeycomb structures, and 3D lattice structures. Further, foams are classified into open-cell foam and closed-cell foam [1]. Cellular materials are widely used for energy absorption because of their ability to absorb energy efficiently at low peak stresses. We encounter many cellular structures in our daily life such as in car seats, helmets, shoe soles, etc.

In nature we find many structures made from more than one material for example, the shell of tortoise, teeth, bones, the tusk of elephant, horn of rhinoceros, etc. Bones, to focus on one example, are made of a soft material – collagen and reinforced with a harder mineral – hydroxy-apatite. The different compositions results in a structure which is resilient to damage. Because of the properties of constituent materials, we get stiffness of the mineral hydroxy-apatite and the energy absorption properties from the softer material collagen. This stiff-soft behavior and the interplay of materials is the inspiration to study energy absorption of multi-material cellular structures in this work.

1.3 Literature Review

Mimicking bio-inspired structures for energy absorption applications has become a promising avenue for study. Biological materials and structures exhibit extraordinary energy absorption capacity and provide inspiration for design of new energy absorbers [4]. Biological structures like nacre, wood, sponge feature unusual mechanical properties that are difficult to reproduce in man-made and artificial materials [5]. In general, energy absorption structures are intentionally shaped

elements fabricated from different types of materials that are designed to disperse the maximum possible value of externally applied energy by transforming it to internal energy via deformation as plastic work [6]. For protection against an impact it has been suggested that it is necessary to develop a cellular structure which shows sufficient auxetic behavior, good strain sensitivity and exhibits tunable stiffness as per the application requirement [7]. Despite recent advances in materials and manufacturing techniques, the design and fabrication of low-cost structural materials with light weight and superior mechanical performances still represents a challenge.

A metamaterial is defined as a material with unprecedented properties not observed in nature [8]. Auxetic materials are a novel class of mechanical metamaterials that have interesting property of negative Poisson's ratio by virtue of their architecture rather than composition. They get shorter in transverse direction when compressed in longitudinal direction and vice versa. A wide range of negative Poisson's ratio can be obtained by varying the geometry and architecture of the cellular materials [7]. Tiantian Li et al. conducted a study on auxetic lattice reinforced composites by exploiting negative Poisson's ratio to design 3D printed composites. They used TangoPlus and VeroWhite – stiff and soft materials, to fabricate the specimens on a Polyjet 3D printing system. In this study, auxetic lattice structures were used as reinforcements and incompressible soft material was employed as matrix. The auxetic lattice reinforced composites have enhanced mechanical performance achieving a unique combination of stiffness and energy absorption, compared with the non-auxetic lattice reinforced composites. This improved

mechanical response was achieved due to the negative Poisson's ratio effect of the auxetic reinforcements [9].

Multi-material additive manufacturing has also shown capability to introduce material gradients in a 3D printed material. In a study performed by Krishna Kumar Saxena et al. multi-material cellular designs are investigated using finite element method. They introduced a material gradient in the cell to tune cellular stiffness as per the specific requirement [7]. Simon R.G. Bates et al. performed a study on density graded 3D printed cellular arrays. They found that by grading the structure, higher total energy in compression than the equivalent uniform array can be achieved [10]. In the work by Amanda L. et al. on study of bi-material lattices, it was found that high strength and straining capability is achieved by incorporating both the geometry and material properties [11]. A study on multilayered cell composite structure composed of hard brittle and soft flexible phases was done by Huan Jiang et al. The design was inspired by the structure of cork. They discovered that a multi-layered architecture can turn brittle catastrophic failure into progressive failure with enhanced energy absorption [5]. M.R. Mansouri et al, performed a study on periodic single material cellular D-structure and the corresponding co-continuous composite. They also had a similar finding. The mechanism of deformation in single cellular structure that experiences instability can be transitioned to a stable deformation in multi-material composite. The soft phase plays a pivotal role for transitioning [12]. In a paper on co-continuous composites by Lifeng Wang et al., the potential to design and fabricate co-continuous glassy polymer and rubbery polymer materials with enhancements in strength, stiffness and energy dissipation using a 3D printer is explained [13]. In

another work on co-continuous composites the quasi-static compressive behaviors of the co-continuous glassy polymer/liquid composites are studied. Due to the presence of liquid filler, the mechanical properties are significantly enhanced [14]. A study on hollow micro-lattices was performed by Yilun Liu et al. Highly energy absorbing nano-porous materials functionalized liquid was incorporated into hollow micro-lattice structures to develop a superior energy absorption system [15]. In a similar study it was found that hollow micro-lattice architectures are very attractive for energy absorption and that hollow tube architecture results in higher energy absorption per weight as compared to foams or solid strut lattice structures [16].

After studying the literature, we realized that there are few studies and few experiments being conducted with direct emphasis on energy absorption. Most of these multi-material cellular structures use periodic design. Most of these studies are performed using the PolyJet technology.

1.4 Research Objectives

The main objective of this research study is to experimentally observe the energy absorption behavior of multi-material cellular structures. We try to find out using experiment and analysis if multi-material cellular structures improve the energy absorption properties. We introduce aperiodicity in our designs and try to study the role of aperiodicity by drawing comparisons between the periodic and aperiodic structures, across the specimens. In the chapter on Design we discuss the software used to design the specimens and how aperiodicity was introduced. In the manufacturing section we see the technology employed to manufacture the specimens, along with the challenges faced and the solutions. Chapter 4 – Testing

describes the process of the specimens were compressed. In the analysis section we see how the data received from testing was converted to energy absorption metrics. We report metrics such as the energy absorbed, and densification strain etc., to find the answers to our proposed research objectives. Finally, the concluding chapters discuss the conclusion and future work. The complete experiment was conducted in four stages – Design, Manufacturing, Testing, Analysis.

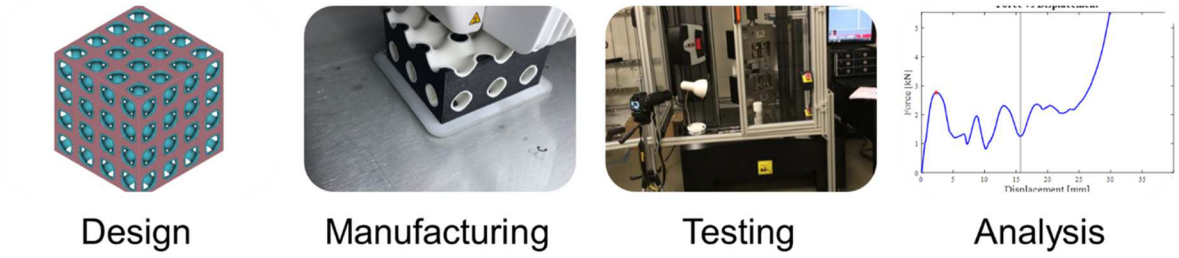

Figure 1 : Approach

CHAPTER 2

DESIGN

2.1 Design Software

For the purpose of designing multi-material cellular structures, two software packages – MATLAB and nTopology, were used. MATLAB was used for creating a code for a set of points which was later imported to nTopology. The point set forms the base for designing the lattices. Aperiodicity is specified given in MATLAB to design the aperiodic cellular structures. Light weight and optimized parts with functional requirements can be created using nTopology Platform [17].

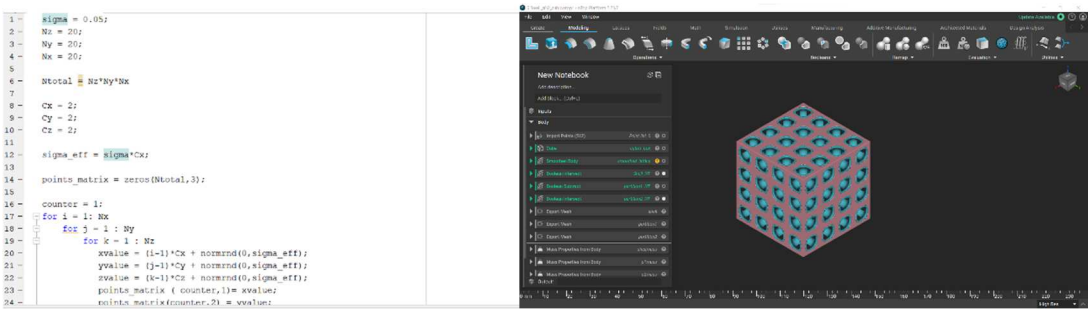

Figure 2 : (a) MATLAB (b) nTopology

2.2 Design Approach

The aperiodic designs were developed using a Voronoi framework. This approach is implemented to create cellular structures that are fully connected without having any material discontinuity. The position of the solid and air phases can be controlled in many ways to adapt the architecture of structures for the required applications [3].

The Voronoi framework subdivides space into a set of sub-spaces according to the distribution of the objects [18]. Each vertex represents the center of a Voronoi cell called the nucleus. An increasing random offset is given to the nuclei of the cells to generate a random structure. Therefore, the cellular solids are formed by nucleation and growth of

the cells. If all the cells nucleate randomly in space and grow at the same linear rate, the resulting structure is a Voronoi structure [19]

There are several methods to create Voronoi Structures with varying randomness like the simple sequential inhibition (SSI) method, nucleus perturbation, node perturbation and cylinder packing. In the SSI method, Voronoi nuclei are created using random X, Y, (and Z in the 3D case) coordinates, with some minimum distance between nuclei. Nuclei that lie too close to each other are deleted and new random coordinates are created. This method follows a poisson distribution. In the nucleus perturbation method, the Voronoi nuclei are created using a periodic pattern and then perturbed by a random vector with a given sigma value. In the node perturbation method, a set of periodic nuclei is created within the given value, and the Voronoi is derived from that point set, and then the nodes of the actual structure are perturbed using a random vector. In cylinder packing a given volume is filled with cylinders or spheres and the center of each cylinder becomes the Voronoi nucleus.

For our experiment, we introduce aperiodicity using the nucleus perturbation method. Three different values of sigma – 0, 0.05, and 0.1 are given to the point sets and the respective structures are derived from the point set. We also introduce the variation in wall thickness – 0.5mm and 1mm, resulting in nine specimens with wall thickness 0.5mm and three variations of sigma, and the other nine with wall thickness 1mm and the same degree of sigma. In total, we design and perform the testing on 18 specimens shown in the figure below.

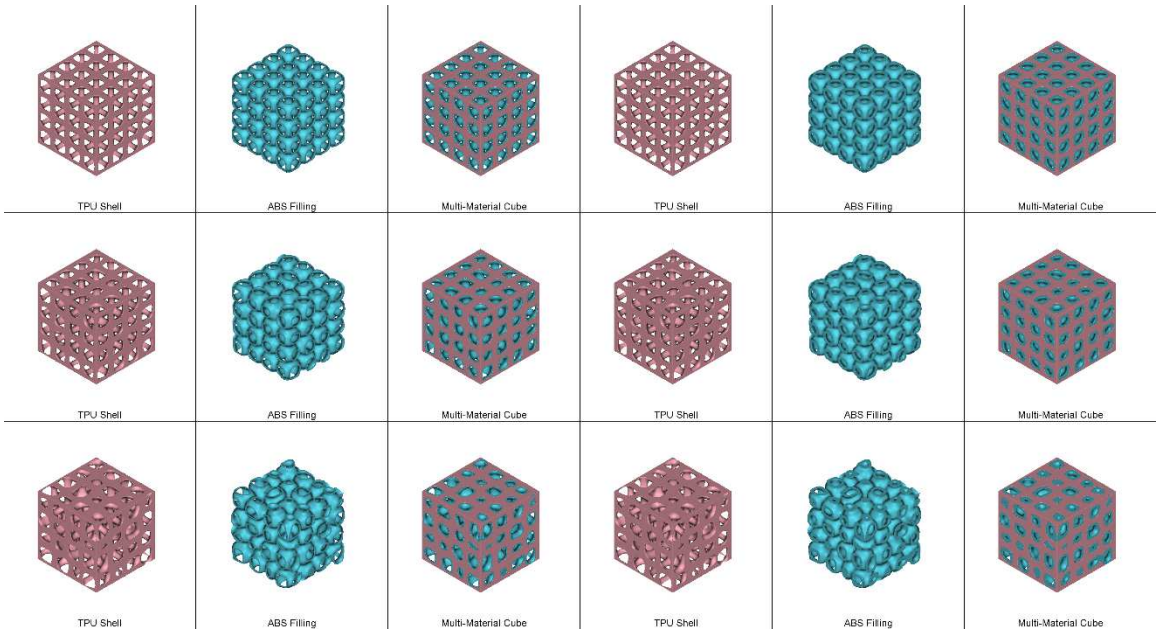

Figure 3 : Design List

2.3 Design Process

The complete design process can be completed in fourteen steps explained below. The figures here show the design process.

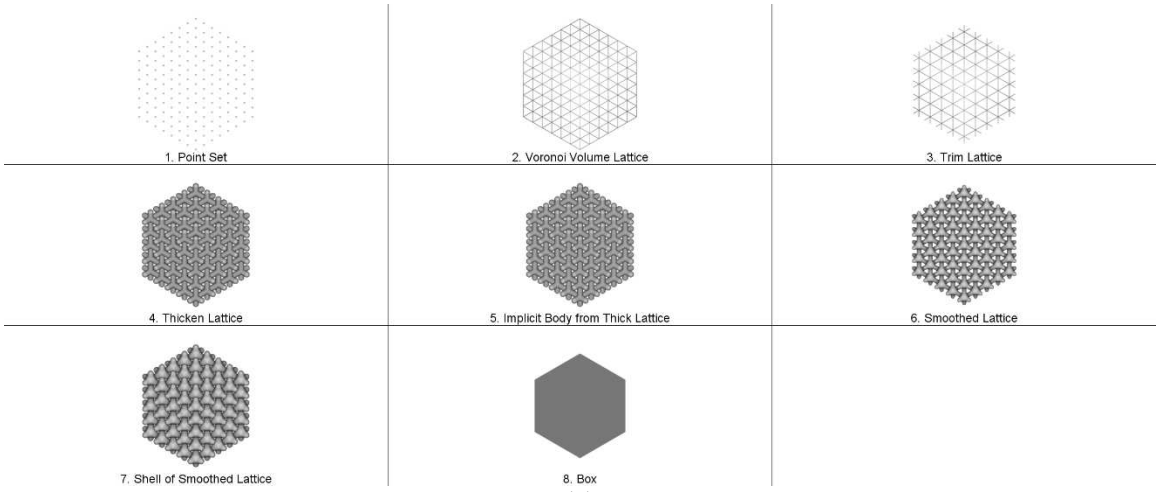

(a)

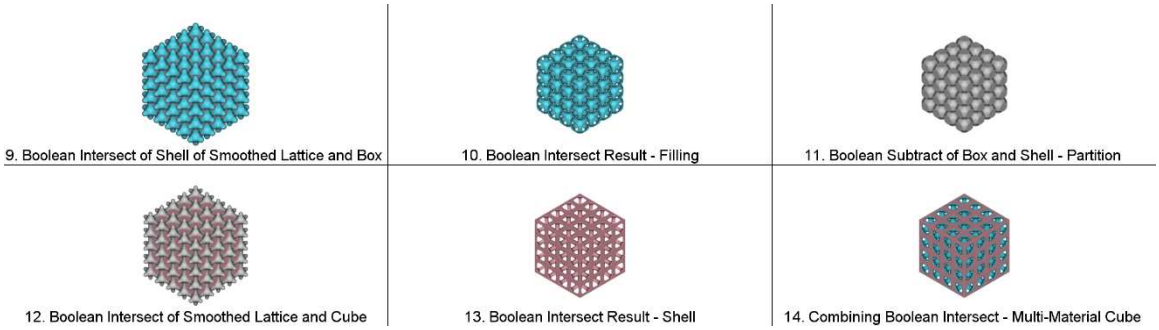

(b)

Figure 4 : (a,b) Design Process

Let us examine the design process step-by-step.

(i) Point Set : First, a point set must be imported into nTopology using the import points feature. These points are the list of points in [X, Y, Z] coordinates and can be periodic or aperiodic. Based on the randomness level of the points, the randomness of the cellular structure can be varied.

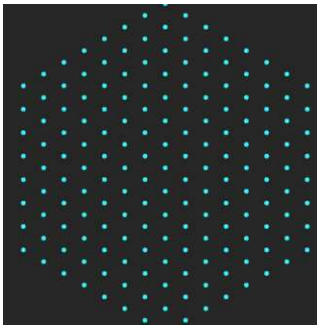

Figure 5 : Point Set

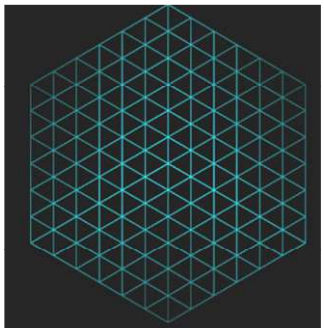

Figure 6 : Voronoi Volume Lattice

(ii) Voronoi Volume Lattice : Once the points are imported in nTopology, a Voronoi volume lattice is generated by using the 3D points as an input.

(iii) Trim Lattice : The edges and sides of the lattice should be as per the dimensions of the design, so the lattice is trimmed to contain the dimensions designed for the specimen.

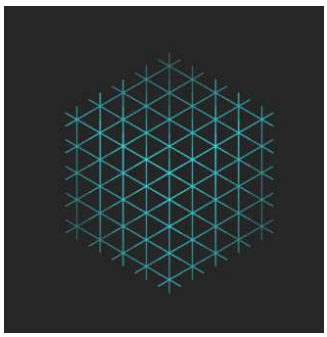

Figure 7 : Trim Lattice

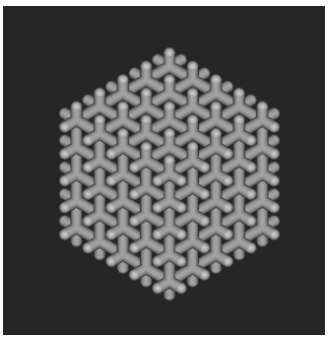

Figure 8 : Thicken Lattice

(iv) Thicken Lattice : The lattice is then thickened. The point density and thickness of the lattice itself will control the relative density of the beam lattice.

(v) Implicit Body from Thick Lattice : Next, we need to convert the lattice into an implicit body in nTopology.

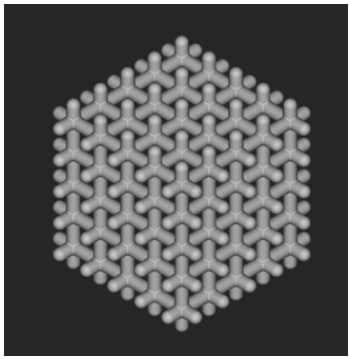

Figure 9 : Implicit Body from Thick Lattice

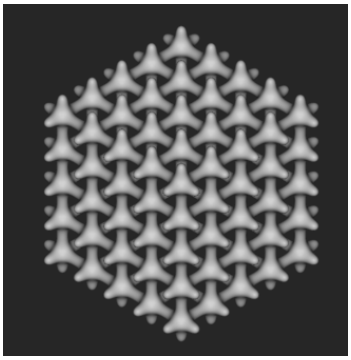

Figure 10 : Smoothed Lattice

(vi) Smoothed Lattice : Now the lattice must be smoothed. The number of smoothing iterations control how smooth the lattice becomes.

(vii) Shell of Smoothed Lattice : Now that the lattice is smoothed, a shell can be created.

(viii) Box : The shell is created but we cannot see it is the shell because the sides are enclosed, so we need to make a box to perform the Boolean intersection operation. The dimension of the box is 40 x 40 x 40 mm.

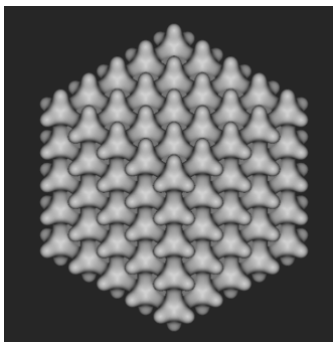

Figure 11 : Shell of Smoothed Lattice

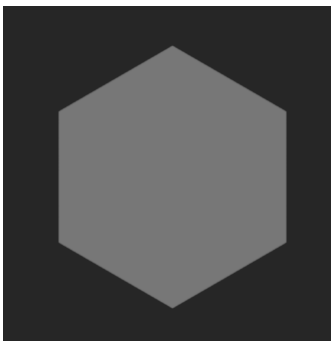

Figure 12 : Box

(ix) Boolean Intersect of Shell of Smoothed Lattice and Box : The box and shell of the smoothed lattice are combined using the Boolean intersect feature in nTopology shown in the figure below.

(x) Boolean Intersect Result – Filling : Boolean intersect operation is performed to generate a shell. The partition generated is named as Filling for the purpose of this study.

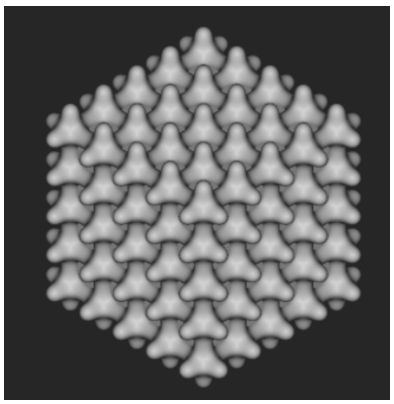

Figure 13 : Boolean Intersect

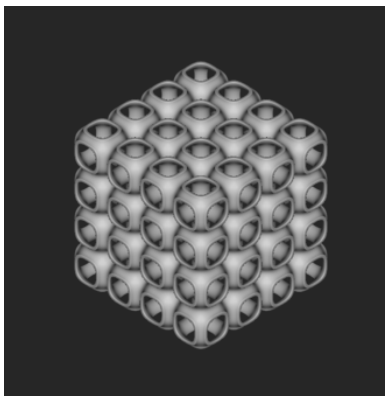

Figure 14 : Filling

(xi) Boolean Subtract of Box and Shell – Negative Space/Empty Space : Boolean intersect of box and shell results in a partition shown below. It is the negative

space between the box and shell. Therefore, for the purpose of this study, it is named as Empty Space.

(xii) Boolean Intersect of Smoothed Lattice and Cube : This Boolean intersection is performed to create a shellular like partition. The figure below shows how the Boolean intersect looks like in nTopology.

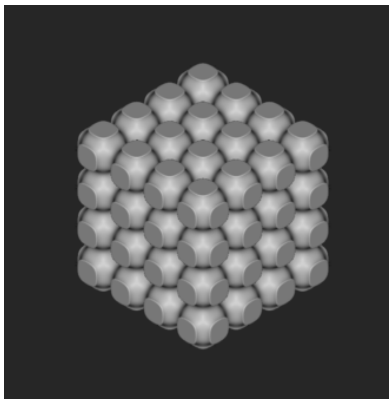

Figure 15 : Negative Space

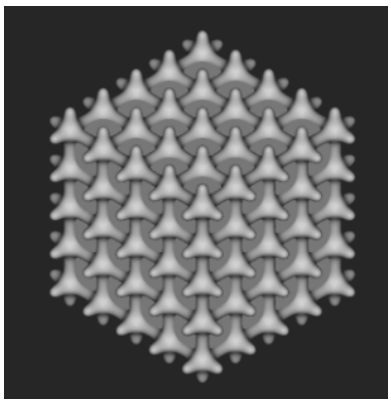

Figure 16 : Boolean Intersect

(xiii) Boolean Intersect Result – Shell : the result of Boolean intersect is partition named Shell for the purpose of this study. It is the negative space besides the Filling and Negative Space.

(xiv) Combining Boolean Intersect – Multi-Material Cube : When the partitions generated as a result of Boolean intersect operations – Shell and Filling are combined, the result is a Multi-Material cube.

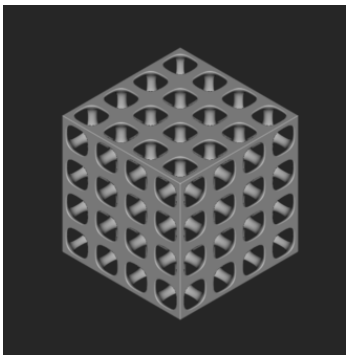

Figure 17 : Shell

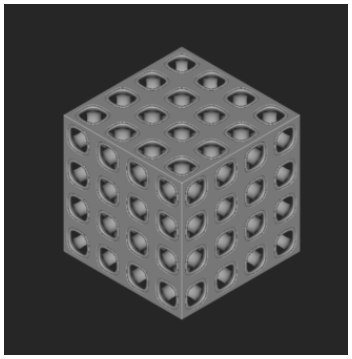

Figure 18 : Combined Cube

After performing the iterative design process, we get three partitions – Shell, Filling and the Empty Space. For this study, we combine the Shell and Filling to form the Multi-Material Cube, shown in the figure below.

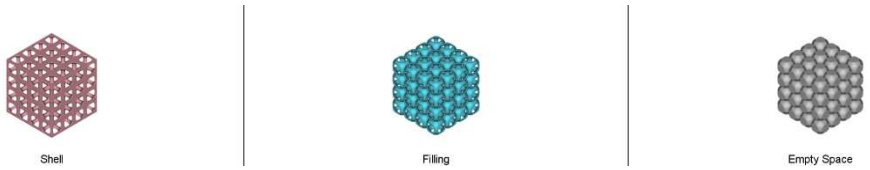

Figure 19 : Partitions

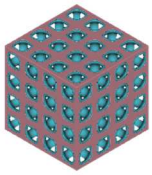

Figure 20 : Multi-Material Cube

2.4 Effect of Wall Thickness

As mentioned, we decided to vary the wall thickness for the specimens – 0.5mm and 1mm. First, let us see the effect of wall thickness on the Filling. There is no effect of wall thickness on the Shell because the thickness is specified on the inside.

(a) (b)

Figure 21 : Effect of Wall Thickness ABS Filling (a) 0.5mm (b) 1mm

Figure 22 : Effect of Wall Thickness TPU Shell

2.5 Effect of Aperiodicity

Aperiodicity in the cellular structures was introduced by offsetting the points by some linear distance. Three values of sigma – 0, 0.05, 0.1 were given. The sigma value is specified to the point set in Matlab and the resulting structures are generated in nTopology. The figures below show the effect of perturbations on Filling, Shell, and Multi-Material Cube.

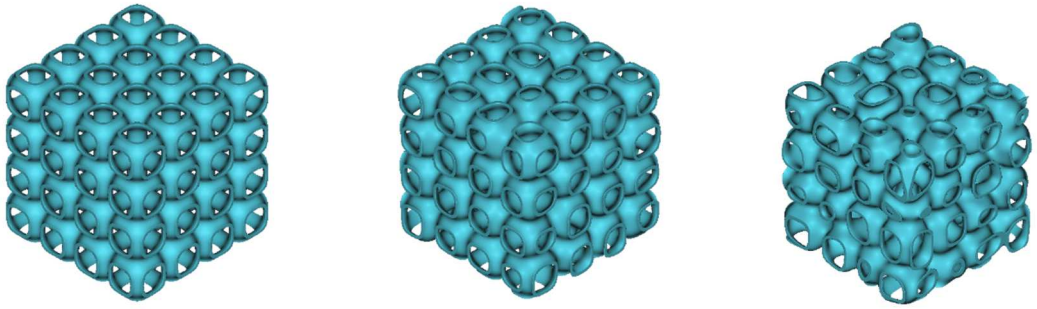

(a) (b) (c)

Figure 23 : Effect of Aperiodicity ABS Filling (a) Sigma 0(b) Sigma 0.05 (c) Sigma 0.1

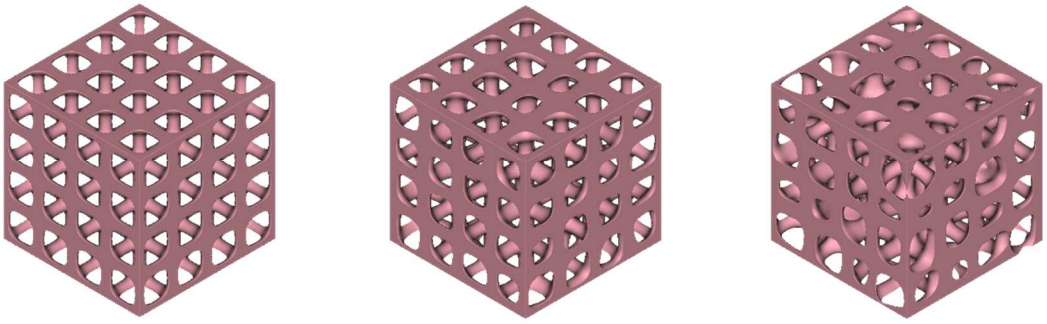

(a) (b) (c)

Figure 24 : Effect of Aperiodicity TPU Shell(a) Sigma 0(b) Sigma 0.05 (c) Sigma 0.1

(a) (b) (c)

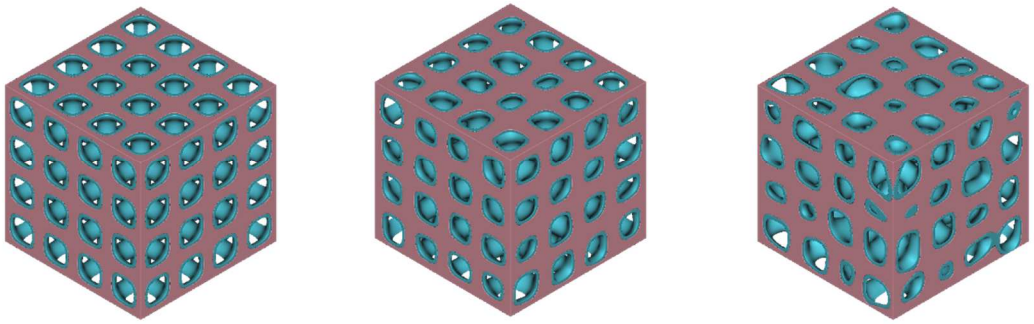

Figure 25 : Effect of Aperiodicity on Multi-Material Cube (a) Sigma 0 (b) Sigma 0.05 (c) Sigma 0.1

CHAPTER 3

MANUFACTURING

3.1 Overview

3D printing or Additive manufacturing is a process where product is directly manufactured from its computer-aided design (CAD) file, layer by layer. In the recent years, 3D printing technology has emerged as a flexible and versatile technique for manufacturing. 3D printing is the opposite of subtractive manufacturing, where excess material is removed to form an object. This tool less manufacturing approach gives new design flexibility and reduces energy use. Main applications of additive manufacturing include rapid prototyping, rapid tooling, direct part production and part repairing of plastic, metal, ceramic and composite materials [20].

The American Society for Testing Materials (ASTM) has characterized 3D printing technologies into seven groups, namely, the binding jetting, directed energy deposition, material extrusion, material jetting, powder bed fusion, sheet lamination and vat photopolymerization [21].

3.2 Technology used for the experiment

For this research, one of the most popular technologies - material extrusion is used. Material extrusion is also known as Fused Deposition Modeling (FDM). The principle of FDM involves surface chemistry, heat energy and layer deposition. The process begins by importing a STL file of a model into a preprocessing software, where it is sliced into horizontal layers typically having thickness on the order of hundreds of microns. After reviewing the path data and generating the tool paths, the data is downloaded to the FDM machine [22]. The time required to print 3D model depends on

the number of layers being printed, vertical height of model rather than the number of models being printed [23].

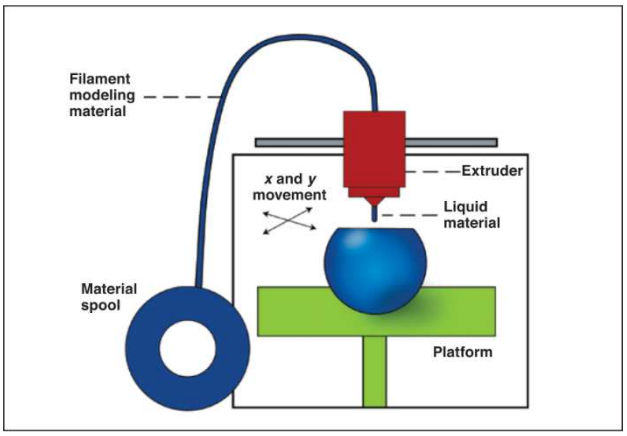

Figure 26 : Fused Deposition Modeling Printer, Christian Groth et al.(2014)

As shown in the above figure, a FDM printer extrudes material through nozzle, by heating it beyond its melting point, depositing it layer by layer [23].

This 3D printing technology can also be used to print muti-materials. FDM systems are widely used in applications, ranging from quick and inexpensive rapid prototyping to tough and rigid parts suitable for end-use [24].

3.3 Printer Used for Manufacturing

The 3D printer used for this research is the Ultimaker S5, a widely available commercial 3D printer. Ultimaker S5 enables dual extrusion for multi-material prints. The printer head comes with two swappable print cores, which helps the user to easily change nozzles depending on the type of print – high speed printing or complex intricate details. This dual extrusion print head has an auto-nozzle lifting system [25]. One of the interesting features of Ultimaker is it comes with a filament flow sensor. This sensor indicates the user if the printer runs out of filament, or gets stuck in the feeder, by

automatically stopping the print jobs. The build volume of the printer is 330 x 240 x 300 mm and it can produce high-quality parts.

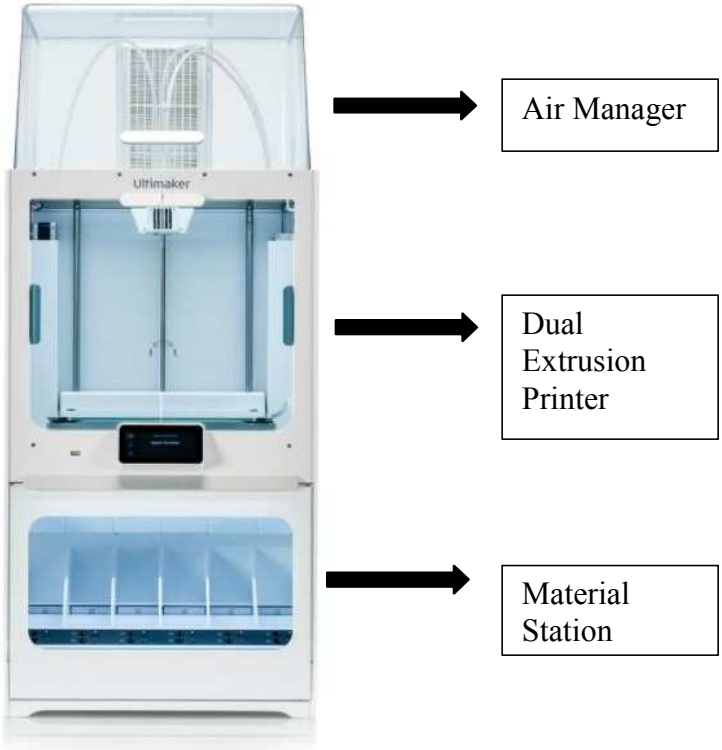

Figure 27 : Ultimaker S5, Ultimaker Website

As illustrated in Figure 27, the printer also has two other components – Ultimaker S5 Air Manager and Ultimaker S5 Material Station. Ultimaker S5 Air Manager is mounted on top of the printer to create a safer printing environment and fully contain the printing process. It completely encloses the open-ended top of printer and also includes an intelligent fan and air filtration system [26].

Ultimaker S5 Material Station is positioned underneath the printer and acts as an automated delivery system and storage unit. One of the advantages of the material station is it controls humidity below 40% protecting the material from degrading and absorbing moisture from environment. It also protects the filament from humidity and dust.

3.4 Material Allocation

For this research, two materials were used. A thermoplastic polymer – Acrylonitrile Butadiene Styrene (ABS) and a thermoplastic elastomer – Thermoplastic Polyurethane (TPU). The focus was to manufacture ABS and TPU together because together they exhibit soft-hard nature. Shell is made from TPU and Filling is made from ABS.

Acrylonitrile Butadiene Styrene (ABS) is a thermoplastic polymer, hard and tough in nature. Like the name suggests it is made up of three monomers : acrylonitrile, butadiene, and styrene. Acrylonitrile a synthetic monomer contributes to the ABS chemical resistance and heat stability. Butadiene delivers toughness and impact strength to ABS. Styrene provides rigidity and processability of ABS plastic [27]. The printing temperature of ABS is relatively low, and it is also a low-cost material which makes it suitable for 3D printing. High rigidity, good impact resistance at low temperatures, good weldability are some of the physical properties of ABS.

Thermoplastic Polyurethane (TPU) is a thermoplastic elastomer with high durability and flexibility. TPU 95A is a semi-flexible material with high durability and flexibility. It has properties between characteristics of plastic and rubber. Excellent tensile strength, high elongation at break and good load bearing capacity are some of the physical properties of TPU. The thermoplastic nature of TPU provides a substantial amount of combination of physical and chemical property combinations. TPU finds its applications in automotive, sports and textile coatings, etc. [28].

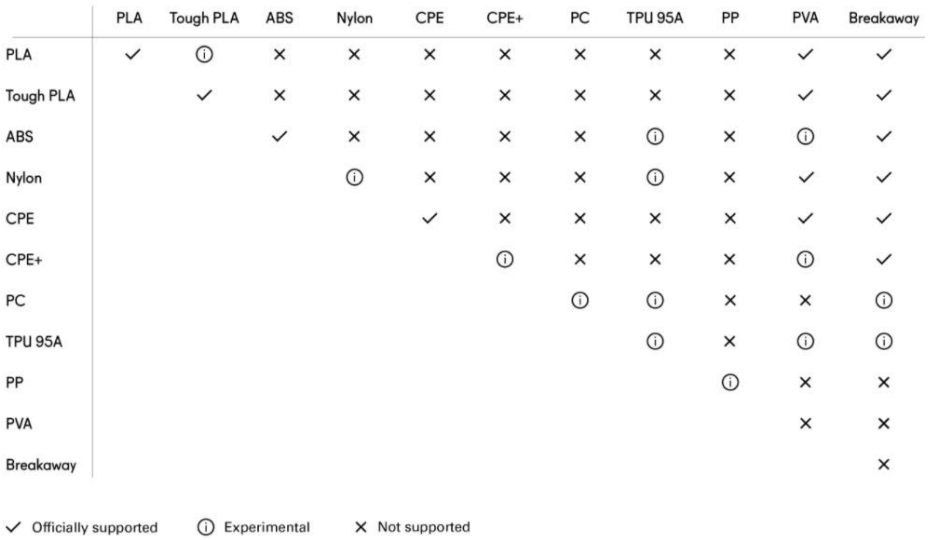

Figure 28: Material Compatibility Chart, Ultimaker Website

The picture above is an overview of possible dual extrusion material combinations supported on Ultimaker S5 [25]. As seen from the compatibility chart, ABS is only compatible with Breakaway material which is a support material. Ultimaker S5 recommends printing ABS with TPU 95A and PVA for experimental purposes. But again PVA is a support material, and it does not bond well with ABS. The only true multi-material combination of ABS with build material is compatible in experimental mode is TPU 95A.

3.5 Manufacturing Pre-Processing Software

Cura is a 3D slicing software from Ultimaker that prepares the 3D model for printing. STL, OBJ, X3D, 3MF, BMP, GIF, JPG and PNG file formats are supported on Cura. Ultimaker Cura optimizes print profiles for Ultimaker 3D printers, but the software will slice 3D files for any 3D printer irrespective of brand and model [29]. As shown in the figure below, the software allows one to open and place multiple models at a time on the print bed allowing for continuous printing.

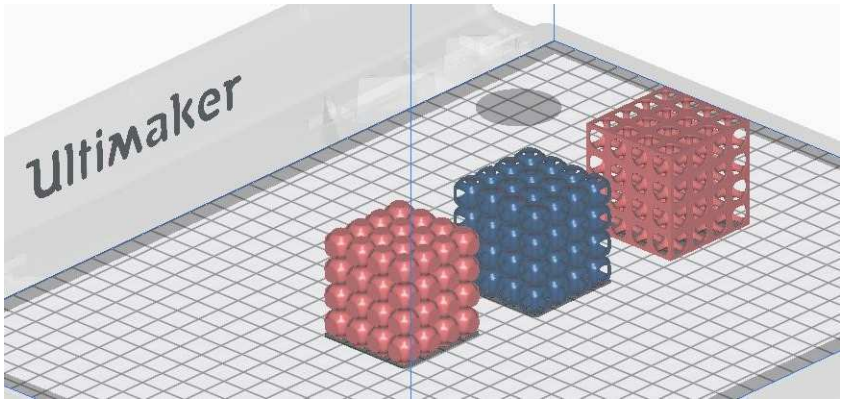

Figure 29 : Pre-Processing Software : Ultimaker Cura

For printing multi-material cellular structures, the models were merged in Ultimaker Cura specifying the material and the extruder using available Ultimaker database. The setting 'Enable Prime Tower' was enabled while preparing the model. Prime tower is the sacrificial tower or an additional print that is created for printing. It helps in switching by preparing the nozzle before printing next layer, as shown in the figure below. For this research, the blue material is the ABS and red (and occasionally black) colored filament is TPU.

To optimize the overall printing, print time and print quality, few settings were changed. Finding the optimal temperature for printing ABS and TPU together was one of the important factors. Another aspect is layer height. Higher values produce faster prints in lower resolution and lower values produce slower prints in high resolution. The layer height along with print speed affects the total print time.

As mentioned earlier all the 18 specimens were printed using a FDM printer – Ultimaker S5. The images below show the multi-material printing, ABS only printing and TPU only prints.

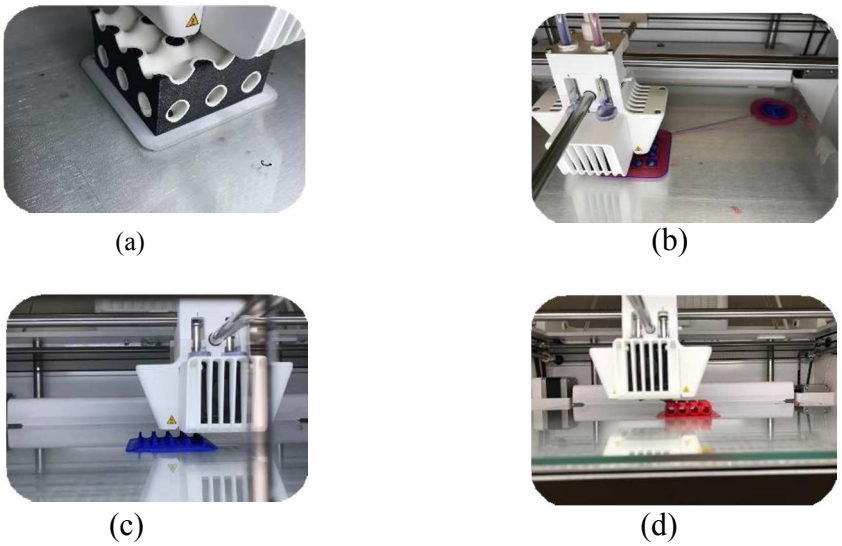

(a) (b)

(c) (d)

Figure 30 : Working of Ultimaker S5 (a,b) Multi-Material Printing (c) ABS only print (d) TPU only print

3.6 Manufacturing Challenges

TPU elastomers are hygroscopic in nature and tend to absorb moisture from the atmosphere and surroundings, degrading over time. Ultimaker states that TPU 95A is prone to oozing and this is one of the reasons it is not recommended to print TPU 95A in combination with other materials since the extrusion process needs to be paused on one head to let the other extrude. Therefore, a relative humidity of below 50% is recommended when printing TPU 95A to limit oozing and prevent moisture absorption. The images below show the effects of humidity on TPU 95A. The three major ones are stringing, clogging and chipping of the filament.

(a) (b) (c)

Figure 31 : Manufacturing Challenges : (a) Stringing (b) Clogging (c) Chipping

3.7 Manufacturing Challenges – Solution

As a cost-effective and efficient solution, a filament dryer – SainSmart eSun eBox 3D printing filament storage box was installed. Before starting the print, the filament was kept in the dryer for 18-20 hours to completely dry. Reusable desiccant packets made from silica were used in the filament dryer and to store the filament. Ultimaker Material Handling Station was also used to control the humidity while printing.

Figure 32 : Filament Dryer

CHAPTER 4

TESTING

4.1 Mechanical Testing of 3D Printed Specimens

This study analyses the mechanical response of cellular structures under large deformations. Quasi-static mechanical testing was performed to identify the deformation mechanisms of the 3D printed cellular structures. The specimens were tested in quasi-static uniaxial compression on Instron 5985 with a load cell capacity of 250 kN. The crosshead displacement of load cell was set to 2.4mm/min. All specimens were compressed till densification was achieved. A DSLR camera was used for recording the compression tests. The Bluehill software connected to the Instron 5985 machine was used to control the machine and acquire force-displacement data. Two rectangular platens were used to transfer the compressive force from load cell. The platens were cleaned with alcohol before each test. Hot air gun was also used to blow out any material residue left behind from pervious tests.

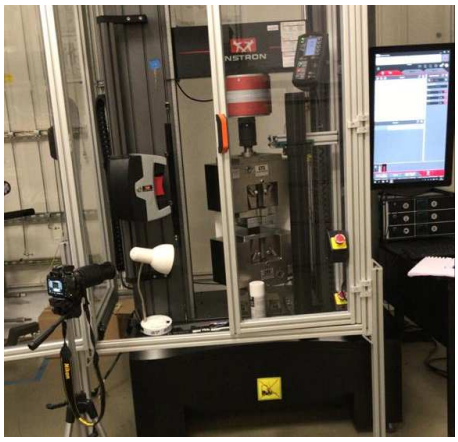

Figure 33 : Compression Testing Setup

CHAPTER 5

ANALYSIS

5.1 Energy Absorption Metrics

The raw force-displacement data obtained from Instron 5985 is converted to energy absorption diagrams. A MATLAB code is created for the analysis. All the metrics are calculated in MATLAB. The force-displacement data from Instron is used as an input and using this data peak stress, densification strain, specific energy absorbed, and energy absorption efficiency are calculated.

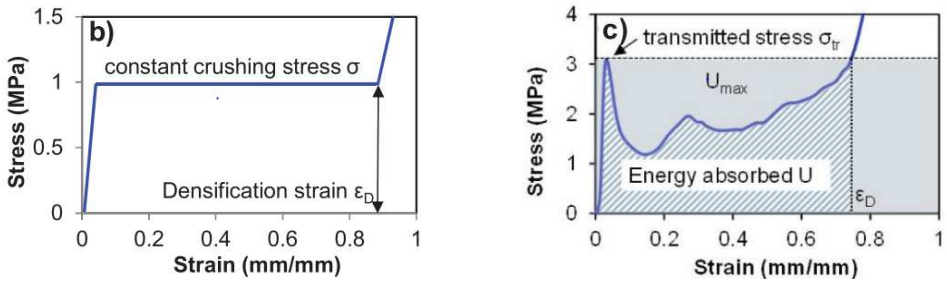

Figure 34 : (a) Ideal energy absorber behavior (b) Actual behavior of cellular structure, Schaedler (2013)

Let us first understand the behavior of an ideal energy absorber and the actual behavior of the cellular structure through this diagram shown above. For an ideal energy absorber, we see a linear region, a flat plateau, and no waviness in the curve. But, if we see the actual behavior of typical cellular structure, we see peaks and valleys in the curve. To understand this behavior better we should first understand some terms.

Initial Peak Crushing Force : It is defined as the peak force at an early stage in the compression process of a structure. This responds to the initiation of cracks in the structure.

Densification Strain : It is the strain value coinciding with the maximum of energy absorption efficiency curve and the goal is to achieve as high as possible.

Energy Absorption (EA) : It is used to evaluate an energy absorber's ability to dissipate the energy through plastic deformation. Energy absorbed is calculated as integral from 0 to densification displacement of force-displacement curve.

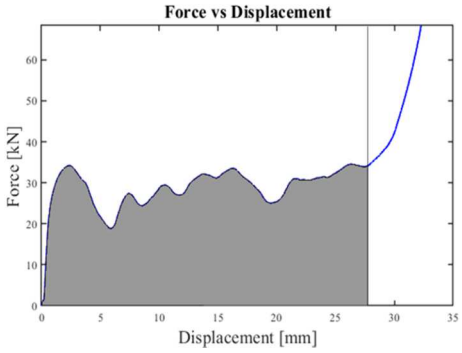

Figure 35 : Energy Absorbed

Specific Energy Absorbed (SEA): The energy absorbed per unit mass gives the specific energy absorbed. SEA is used to compare the energy-absorbing ability of different materials and structures [4].

Maximum energy absorbed : Transmitted stress defines maximum possible energy absorption, for an ideal energy absorber [30].

Energy absorption efficiency : Ratio of usable energy absorbed to the maximum possible energy absorption observed till transmitted stress is exceeded.

In an article by L.J. Gibson, the mechanical response of solids in compression can be characterized by three distinct regimes of behavior : an initial linear elastic region associated with bending edges in open-cell foams and stretching faces in closed-cell foams; a rough constant plateau stress corresponding to cell collapse by buckling, yielding or fracture and extending up to large strains (typically 70-80%) ; and a final

sharp increase in stress corresponding to densification of the material, with opposing cell faces compressed against each other [31].

A constant stress plateau which can correspond to either buckling (elastomeric materials), yielding (metals) and brittle crushing (ceramics). Significant waviness in the stress plateau tends to be related to fracture of individual cell walls [2].

5.2 Energy Dissipation Mechanisms

For the specimen with wall thickness 0.5mm and sigma 0, the force displacement graphs for ABS Filling, TPU Shell and Multi-Material Cube is shown below. For ABS we see how wavy the graph is with lots of peaks and valleys. The graph of TPU is comparatively smoother with one good peak stress. But, for the graph of multi-material specimen we only have one peak, a drop and densification. The peaks correspond to the initiation of deformation – catastrophic failure follows, resulting in sudden loss of load bearing capability until the load is transferred to another set of cells.

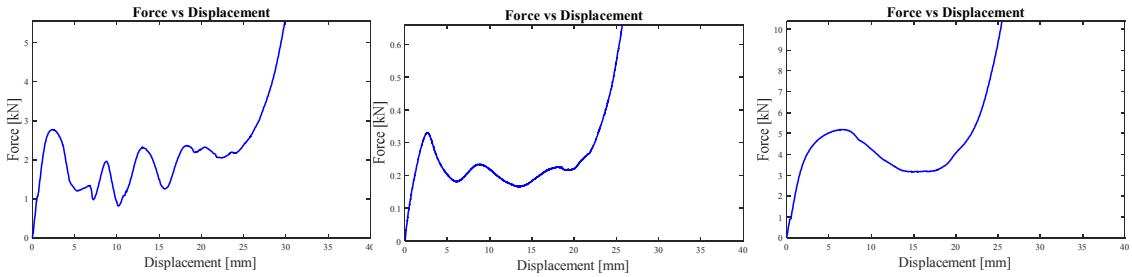

(a) (b) (c)

Figure 36 : Force-Displacement graph of specimen with wall thickness 0.5mm, Sigma 0

(a) ABS Filling (b) TPU Shell (c) Multi-Material Cube

Let us consider another specimen with wall thickness 0.5mm and sigma 0.05. The same force-displacement graphs for the three specimens are shown below. Again, for ABS specimen we see lots of peak valleys. For TPU, we have one peak and a plateau type region. For multi-material specimen, the graph is similar to that of an ideal energy absorber. The efficiency curve for ABS has peaks and valleys. But, for TPU the curve is smoother, and it is even smoother for multi-material specimens. Of these three specimens, the multi-material cube has the highest specific energy (3.32 J/g) and the highest energy absorption efficiency (79.92%).

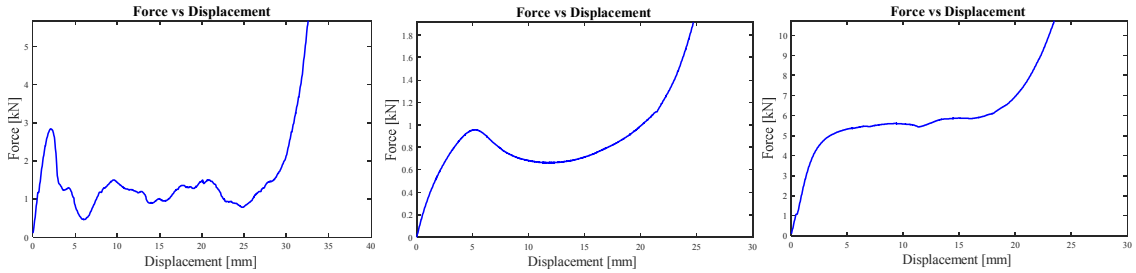

Figure 37 : Force-Displacement graph of specimen with wall thickness 0.5mm, Sigma 0.05 (a) ABS Filling (b) TPU Shell (c) Multi-Material Cube

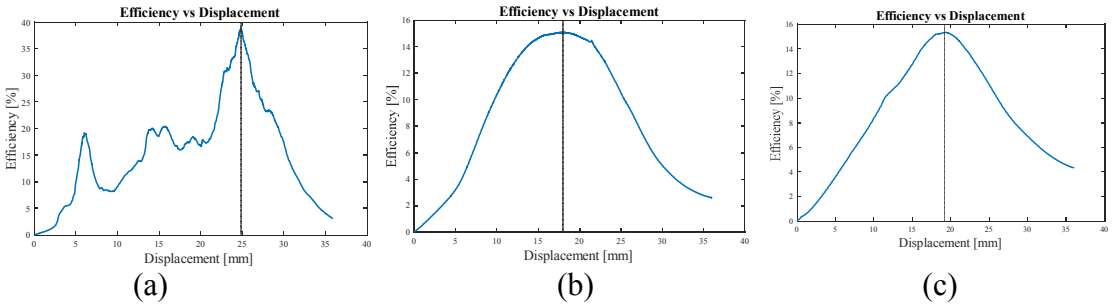

Figure 38 : Efficiency – Displacement graph of specimen with wall thickness 0.5mm, Sigma 0.05 (a) ABS Filling (b) TPU Shell (c) Multi-Material Cube

One may ask where this energy is being dissipated. When the specimen is loaded, work is done by the forces applied to it. Relatively little energy is absorbed in the short, linear-elastic region. The plateau corresponds to the cell collapse by either buckling, yielding, or crushing, allowing large energy absorption at constant loads. The plateau slope depends on the material, the cellular design, and relative density of the cellular structure. The relevant mechanisms for a particular specimen depends on the behavior of the cell-wall material and whether the cells are open or closed [2].

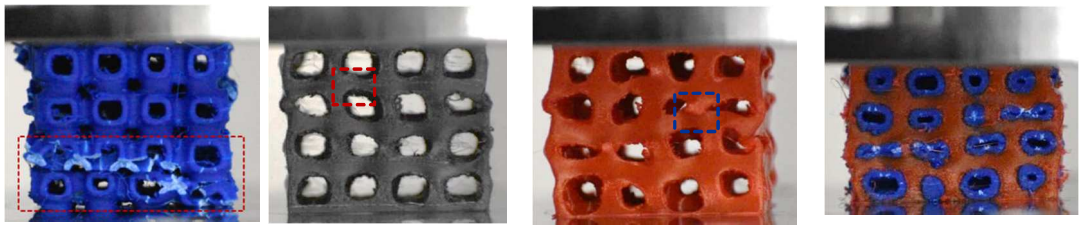

(a) (b) (c) (d)

Figure 39 : Energy Dissipation Mechanisms : (a) Yielding and fracture in ABS (b,c) Wall buckling and wall tearing in TPU (d) Multi-Material Cube

In ABS specimens, yielding and fracture is commonly seen. Two energy dissipation mechanisms are observed in TPU, wall buckling, commonly seen in TPU and wall tearing, which is occasionally seen. In multi-material specimens, the dominant failure mechanism is of ABS - yield and fracture but it is mitigated by the encasing of TPU.

5.3 Effect of Multi-Material on Periodic specimens

The force-displacement graphs for specimens with wall thickness 0.5mm and 1mm with sigma 0 for all three partitions i.e., the shell, filling and the multi-material cube are shown below. We see that the graphs of ABS have lesser waviness, even less for TPU

and the curve is even smoother for multi-material cubes. We see that the graphs start to flatten and there is a rise in plateau for multi-material specimen with wall thickness 1mm.

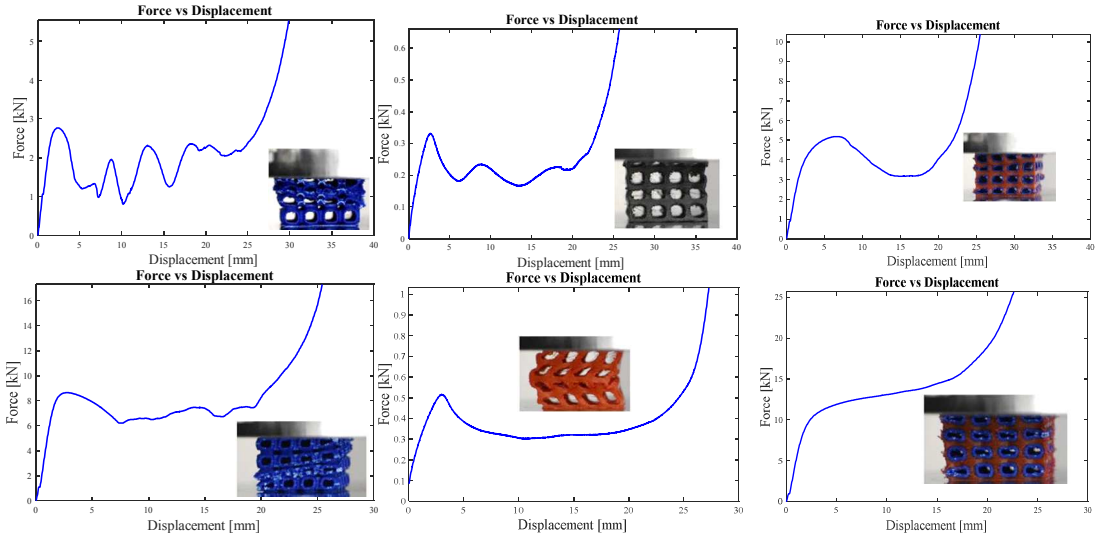

Figure 40 : Effect of Multi-Material on Periodic Specimens

5.3 Effect of Aperiodicity

Aperiodicity effects are discussed in this section for each of the separate compositions used in the study.

(i) ABS Filling : Let us look at the force-displacement graph for all the six ABS specimens. In the first row we have graphs for specimens with wall thickness 0.5mm and the next row has graphs for specimens with wall thickness 1mm. The values of sigma are 0, 0.05, and 0.1. From left to right, in the first row, we see that the curve starts to smoothen as the structure becomes aperiodic. But, for 1mm wall thickness, the effect is less obvious, as it first increases, then drops and later recovers. If we compare just the specimens with same sigma and the different wall thickness, the curve becomes smoother as the thickness increases. Therefore, we can conclude that aperiodicity generally tends to

smoothen ABS plateau, and the same effect is al so seen for higher thicknesses.

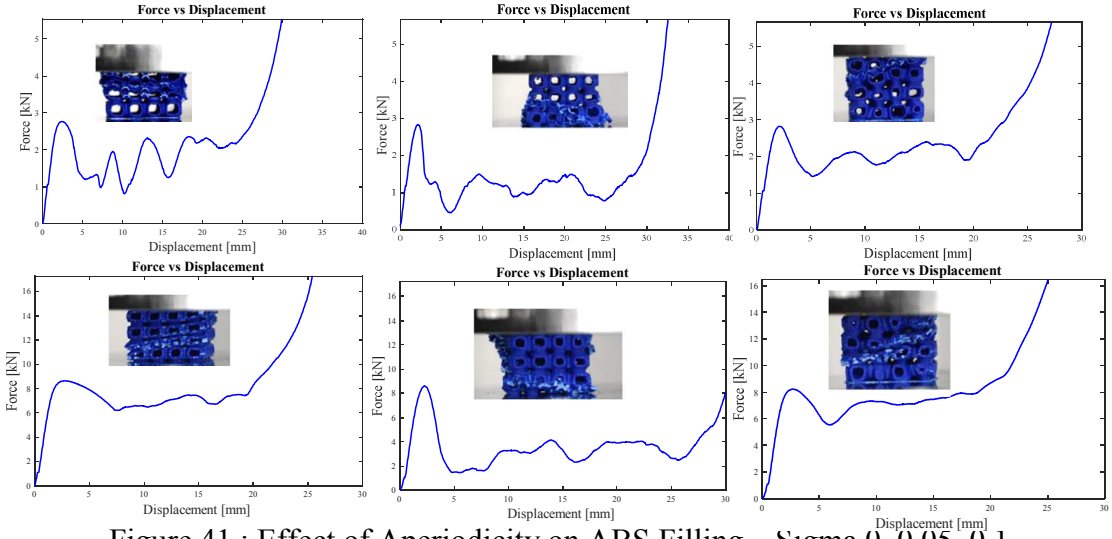

Figure 41 : Effect of Aperiodicity on ABS Filling – Sigma 0, 0.05, 0.1

(ii) TPU Shell : The force-displacement graphs for all the six TPU specimens is shown below. No significant effect of a periodicity on TPU shell can be seen.

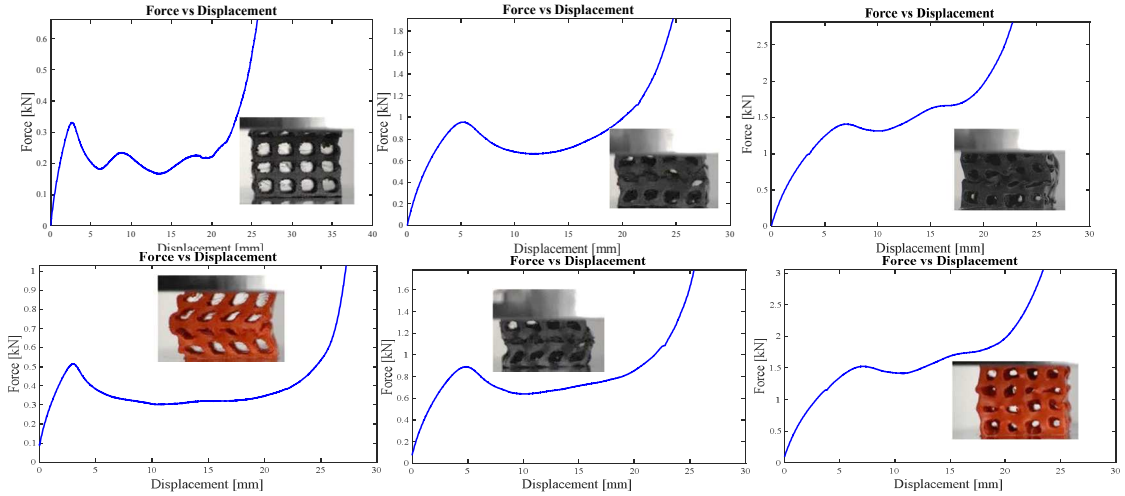

Figure 42 : Effect of Aperiodicity on TPU Shell – Sigma 0, 0.05, 0.1

(iii) Multi-Material Cubes : The force-displacement graphs for all the six specimens are arranged with rows showing the wall thickness 0.5mm and 1mm, in increasing perturbations. A general trend of smoothening of the curve is seen forming the plateau. The shape of the plateau does not change much

but the plateau slope increases. Therefore, aperiodicity tends to smoothen plateau, but effect is only visible up to a certain thickness. Increasing

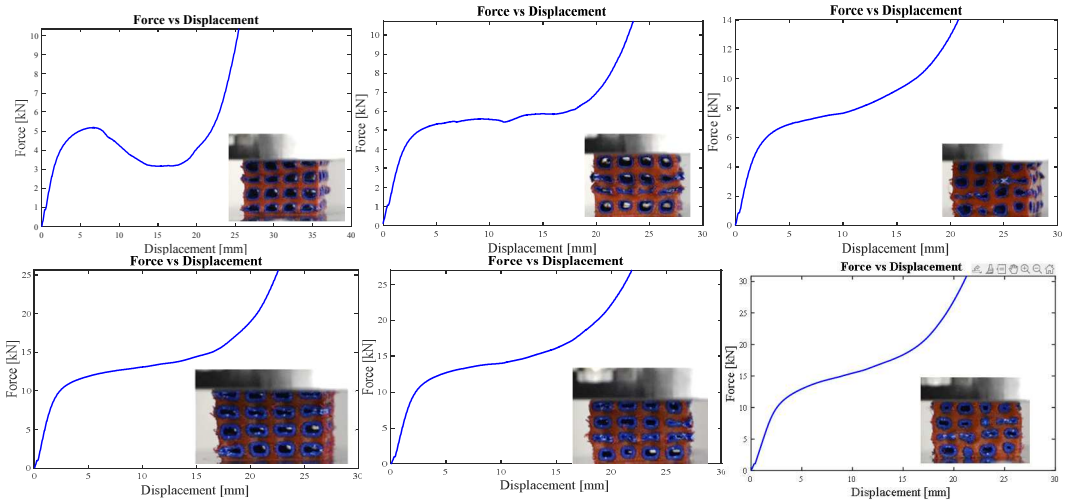

aperiodicity tends to increase in plateau slope. Sigma 0 has lesser plateau slope compared to the specimen with sigma 0 .1.

Figure 43 : Effect of Aperiodicity on Multi-Material Cube – Sigma 0,0.05,0.1

5.4 Specific Energy Absorbed – Comparison

The bar chart below shows that on average the Specific Energy Absorption (SEA) is higher for multi-material specimens. The highest increase in SEA is seen in the specimens with sigma 0.05, for both the variation of wall thicknesses – 0.5mm and 1mm. 44% increase can be seen in specimens with wall thickness 0.5mm and 75% in wall thickness 1mm specimens, over ABS.

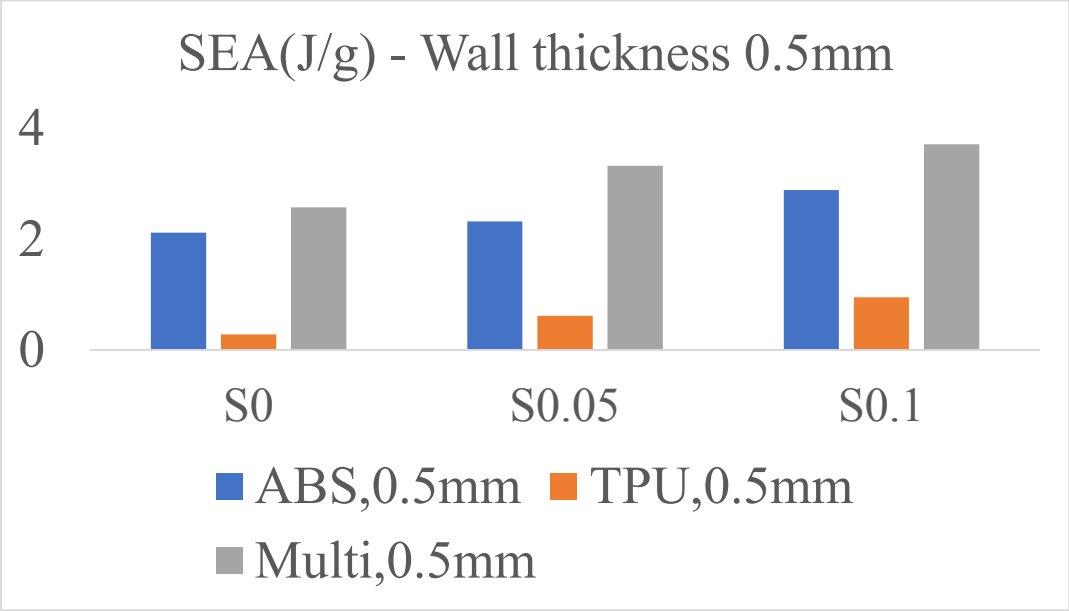

(a)

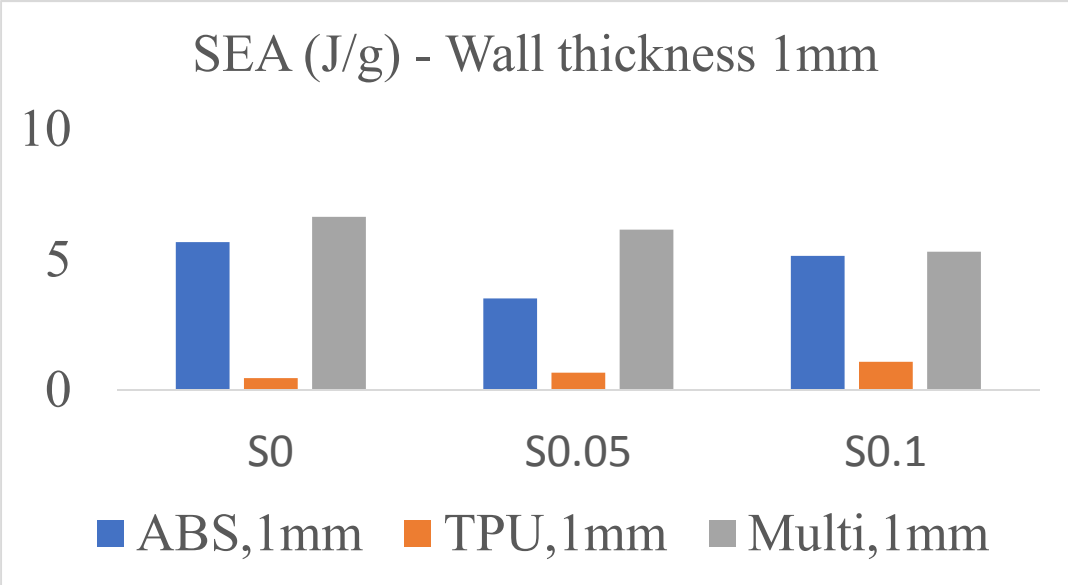

(b)

Figure 44 : SEA of specimens (a) Wall Thickness 0.5mm specimens (b) Wall Thickness 1mm specimens

CHAPTER 6

DISCUSSION

6.1 Why do Multi-Material Cellular Structures have Higher SEA?

To understand this let us look at stress-strain graph of the specimen with wall thickness 0.5mm and sigma 0.05. The blue line represents ABS specimen, red line is for TPU and the green line represents multi-material. The relative density of ABS is 0.16, TPU is 0.27 and the multi-material has the highest density 0.43. For ABS we have one peak, a plateau type region and densification. For TPU we do not see any evident peak, and a plateau type region is seen. For multi-material cube the densification is early at around 0.49 densification strain. But that can be compensated with even higher peak stress then ABS and a higher plateau stress. All these factors result in higher SEA. The high peak stress and early densification in turn are a result of higher relative density for multi-material cellular structures.

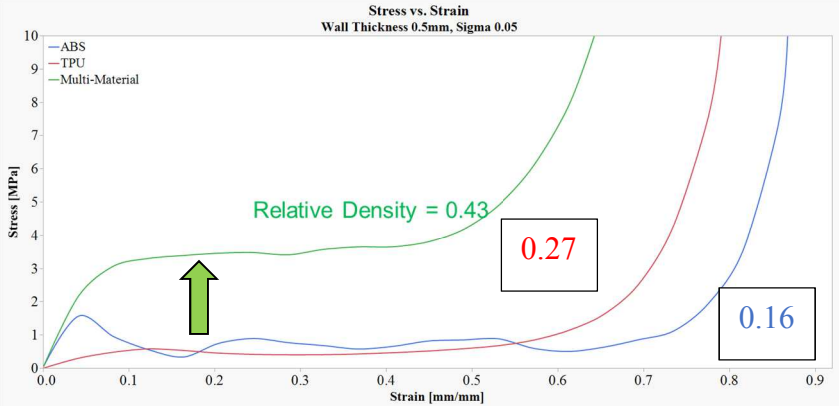

Figure 45 : Stress-Strain graph of specimen with wall thickness 0.5mm, sigma 0.05

This can also be understood by looking at how these specimens fail. The peaks and valleys in the graph correspond to the individual cell wall failures in ABS. In TPU the vertical edge struts buckle first followed with the formation of horizontal failure

bands. Further compression of TPU specimens either tends to rotate or fold them. In multi-material specimens the catastrophic failure is mitigated by elastomeric TPU. The softer material, here TPU helps to turn the instable catastrophic failure into stable progressive failure resulting in higher energy absorption compared to the single material counterparts.

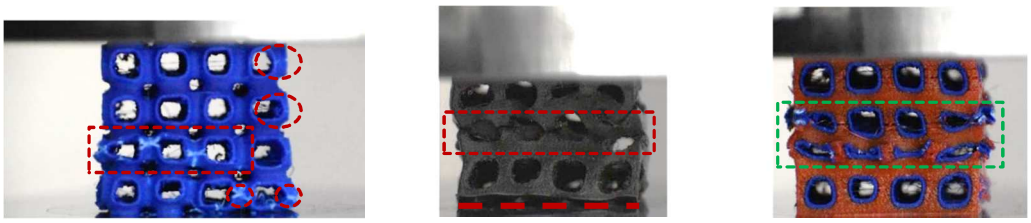

Figure 46 : Failure mechanism in ABS Filling, TPU Shell, Multi-Material Cube

6.2 Effects of Aperiodicity on SEA

The variability chart for SEA is shown below. We observe that aperiodicity increases SEA for 0.5mm thickness but it has the opposite effect for 1mm thickness. For multi-material specimens we see a similar trend, increasing for 0.5mm thickness and decreasing for 1mm thickness. There are two likely explanations for this: SEA increases with relative density up to a point and secondly that the densification drops with relative density. The force-displacement graphs for the six multi-material specimens are shown below. The specimen with wall thickness 0.5mm and sigma 0 has the lowest relative density (0.35) and the specimen with wall thickness 1mm and sigma 0.1 has the highest relative density (0.66). The curves are smoothening and less wavy as the relative density increases. Having said this, from an application standpoint, multi-material specimen with wall thickness 0.5mm and sigma 0.05 is the only specimen that resembles the behavior close to the ideal energy absorber. As the relative density increases, the material increases resulting in higher SEA. This higher energy absorption is achieved at the cost of increase

in plateau slope, which is not desirable for a good energy absorber. As the peak stress is reached, the cube is already compressed and reaches densification and a plateau stress itself is compromised.

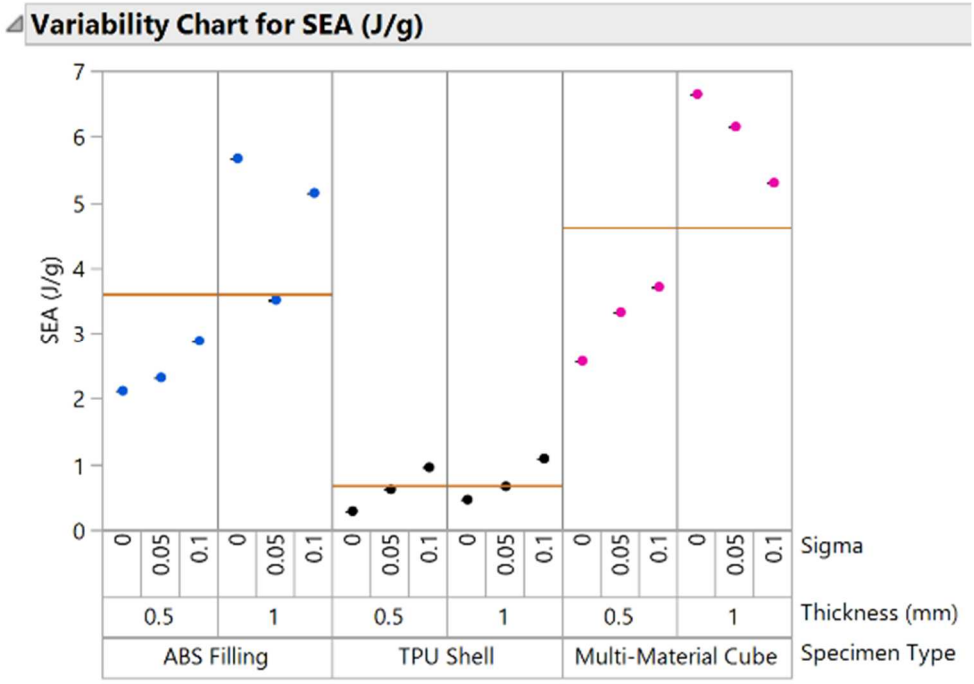

Figure 47 : SEA variability chart

CHAPTER 7

CONCLUSIONS AND FUTURE WORK

7.1 Conclusions

After performing these experiments, we can conclude that SEA is higher in multi-material structures than their individual counterparts, by which we agree with others in the literature. This work also demonstrates that it is possible to use ABS and TPU in dual extrusion systems to fabricate surface-based cellular structures. Aperiodicity improves multi-material SEA further, but only up to a certain relative density.

7.2 Future Work

If we were to repeat the same experiment again, we would try to design the specimens with lower relative density to enable higher densifications. To further understand the stress distribution and energy dissipation, we will be doing Digital Image Correlation (DIC) on the multi-material specimens and performing FEA simulations to relate energy dissipations for different materials. Finally, instead of comparing the multi-material structures to the ABS and TPU base structures that is comprised of, it may be more appropriate to compare it to identical designs constructed entirely out of ABS and TPU, wherein relative densities would be identical and contributions of relative density could be isolated. Finally, it might be of interest to conduct the same experiment by

inversing the material allocation, i.e., ABS Shell, TPU Filling and the corresponding multi-material cube.

REFERENCES

[1] Tang, Y., and Zhao, Y. F., 2016, "A Survey of the Design Methods for Additive Manufacturing to Improve Functional Performance," Rapid Prototyp. J., **22**(3), pp. 569–590.

[2] Gibson, L., and Ashby, M., 1999, *Cellular Solids: Structure and Properties*.

[3] Using, M., Monte, V., and Approach, C., 2019, "Designing Cellular Structures for Additive."

[4] Ha, N. S., and Lu, G., 2020, *A Review of Recent Research on Bio-Inspired Structures and Materials for Energy Absorption Applications*, Elsevier Ltd.

[5] Jiang, H., Barbenchon, L. Le, Bednarcyk, B. A., Scarpa, F., and Chen, Y., 2020, "Bioinspired Multilayered Cellular Composites with Enhanced Energy Absorption and Shape Recovery," Addit. Manuf., **36**.

[6] Kucewicz, M., Baranowski, P., Małachowski, J., Popławski, A., and Płatek, P., 2018, "Modelling, and Characterization of 3D Printed Cellular Structures," Mater. Des., **142**, pp. 177–189.

[7] Saxena, K. K., Das, R., and Calius, E. P., 2017, "3D Printable Multimaterial Cellular Auxetics with Tunable Stiffness," arXiv, pp. 1–18.

[8] Kshetrimayum, R. S., 2004, "A Brief Intro to Metamaterials," IEEE Potentials, **23**(5), pp. 44–46.

[9] Li, T., Chen, Y., Hu, X., Li, Y., and Wang, L., 2018, "Exploiting Negative Poisson's Ratio to Design 3D-Printed Composites with Enhanced Mechanical Properties," Mater. Des., **142**, pp. 247–258.

[10] Bates, S. R. G., Farrow, I. R., and Trask, R. S., 2016, "3D Printed Elastic Honeycombs with Graded Density for Tailorable Energy Absorption," Act. Passiv. Smart Struct. Integr. Syst. 2016, **9799**(April 2016), p. 979907.

[11] Ruschel, A. L., and Zok, F. W., 2020, "A Bi-Material Concept for Periodic Dissipative Lattices," J. Mech. Phys. Solids, **145**, p. 104144.

[12] Mansouri, M. R., Montazerian, H., Schmauder, S., and Kadkhodapour, J., 2018, "3D-Printed Multimaterial Composites Tailored for Compliancy and Strain Recovery," Compos. Struct., **184**(December 2016), pp. 11–17.

[13] Wang, L., Lau, J., Thomas, E. L., and Boyce, M. C., 2011, "Co-Continuous Composite Materials for Stiffness, Strength, and Energy Dissipation," Adv. Mater., **23**(13), pp. 1524–1529.

[14] Liu, Y., and Wang, L., 2015, "Enhanced Stiffness, Strength and Energy Absorption for Co-Continuous Composites with Liquid Filler," Compos. Struct., **128**, pp. 274–283.

[15] Liu, Y., Schaedler, T. A., Jacobsen, A. J., Lu, W., Qiao, Y., and Chen, X., 2014, "Quasi-Static Crush Behavior of Hollow Microtruss Filled with NMF Liquid," Compos. Struct., **115**(1), pp. 29–40.

[16] Evans, A. G., He, M. Y., Deshpande, V. S., Hutchinson, J. W., Jacobsen, A. J., and Carter, W. B., 2010, "Concepts for Enhanced Energy Absorption Using Hollow Micro-Lattices," Int. J. Impact Eng., **37**(9), pp. 947–959.

[17] 2021, "Next-Generation Design & Engineering Software | NTopology," nTopology [Online]. Available: https://ntopology.com/. [Accessed: 14-Apr-2021].

[18] Coates, P., Derix, C., Krakhofer, I. S. P., and Karanouh, A., 2005, "Generating Architectural Spatial Configurations. Two Approaches Using Voronoi Tessellations and Particle Systems," East, pp. 1–18.

[19] Zhu, H. X., and Windle, A. H., 2002, "Effects of Cell Irregularity on the High Strain Compression of Open-Cell Foams," Acta Mater., **50**(5), pp. 1041–1052.

[20] Duda, T., and Raghavan, L. V., 2016, "3D Metal Printing Technology," IFAC-PapersOnLine, **49**(29), pp. 103–110.

[21] Shahrubudin, N., Lee, T. C., and Ramlan, R., 2019, "An Overview on 3D Printing Technology: Technological, Materials, and Applications," Procedia Manuf., **35**, pp. 1286–1296.

[22] Chartier, T., and Badev, A., 2013, *Rapid Prototyping of Ceramics*, Elsevier.

[23] Groth, C., Graham, J. W., and Redmond, W. R., 2014, "Three-Dimensional Printing Technology," **XLVIII**(8), pp. 475–485.

[24] Najmon, J. C., Raeisi, S., and Tovar, A., 2019, *Review of Additive Manufacturing Technologies and Applications in the Aerospace Industry*, Elsevier Inc.

[25] "Professional 3D Printing Made Accessible | Ultimaker" [Online]. Available: https://ultimaker.com/. [Accessed: 14-Apr-2021].

[26] "Ultimaker S5 Pro Bundle: Review the Specs | All3DP."

[27] "Acrylonitrile Butadiene Styrene (ABS Plastic): Uses, Properties & Structure" [Online]. Available: https://omnexus.specialchem.com/selection-guide/acrylonitrile-butadiene-styrene-abs-plastic. [Accessed: 14-Apr-2021].

[28] "Thermoplastic Polyurethane (TPU) Material: Properties & Applications" [Online]. Available: https://omnexus.specialchem.com/selection-guide/thermoplastic-polyurethanes-tpu. [Accessed: 14-Apr-2021].

[29] "Cura Slicing Software – The CREATE Education Project Ltd" [Online]. Available: https://www.createeducation.com/software/cura/. [Accessed: 14-Apr-2021].

[30] Schaedler, T. A., Ro, C. J., Sorensen, A. E., Eckel, Z., Yang, S. S., Carter, W. B., and Jacobsen, A. J., 2014, "Designing Metallic Microlattices for Energy Absorber Applications," Adv. Eng. Mater., **16**(3), pp. 276–283.

[31] Gibson, L. J., and Editor, G., 2018, "C Ellular Solids," (APRIL 2003), pp. 270–274.

BIOGRAPHICAL SKETCH

Rajeshree Varma was born in Ahmedabad, India on May 3,1996. She received her education at Best High School. In 2014, Rajeshree entered Silver Oak College of Engineering and Technology to pursue her Bachelor's in Mechanical Engineering. While doing her bachelor's she had the opportunity to do internship at Indian Institute of Technology, Guwahati. In December 2018, she moved to the United States and started her master's journey in January 2019 at Arizona State University. On April 16, 2021 she successfully defends this thesis and graduates from ASU on May 3,2021. Rajeshree wishes to further her education by pursuing a PhD degree in Mechanical Engineering.